ON THE GEOMETRY OF AXISYMMETRIC VESICLES

BORISLAV ANGELOV and IVAÏLO M. MLADENOV

Institute of Biophysics, Bulgarian Academy of Sciences,
Acad. G. Bonchev Street, Block 21, 1113 Sofia, Bulgaria

Abstract. Vesicle shapes with axial symmetry are modeled using Cassinian oval which when rotated leads to variety of surfaces specified as the level sets of algebraic function. A continuous set of shapes including sphere, torus, biconcave discocyte and dumbbell are described by considering Cassinian oval with a focus distance that is a purely imaginary number. Although these surfaces are not exact solutions of the vesicle shape equation, they reveal some qualitative geometric properties that are difficult to examine by currently available numerical or exact solutions. Relation between the volume of the vesicle at constant surface area and homogeneity index is derived. Going from the implicit to the explicit coordinatization of these surfaces, their fundamental forms and curvatures are found in a form convenient for experimentalists. The integrals specifying the volume and surface area are evaluated analytically in a form relevant to the sphere geometry. The free energy corresponding to bending of outer membrane of the vesicles, modeled by the Cassinian oval, is plotted numerically as a function of the form factor or the reduced volume. The effect of the so called Helfrich spontaneous curvature on the energy minimization is also examined.

1. Introduction

Although the description of vesicle shapes have been a subject of a research interest for a long time (cf. Seifert and Lipowsky [18] for quite representative but still unexhaustive review), the available up to now explicit analytical solutions of the vesicle shape equation are only seven (cf. Ou-Yang *et al.* [15]). This can be related mainly to the fact that we are dealing with a rather complicated differential equation that is not well studied in mathematics. Quite recently, a solution in the case of axisymmetric vesicles has been found which can describe a continuous set of shapes, from red blood cell biconcave discocyte to ellipsoid, sphere, and capped cylinder (cf. Liu *et al.* [13]). Looking closely at

this solution a natural question arise about the lack of appropriate coordinates for dumb-bell type vesicles.

One possible way to answer this question could be a discovery of a solution of axisymmetric vesicle shape equation in spherical polar coordinates. Since this is still a formidable task, our attention is concentrated on approximate analytical description based on the well-known model of red blood cell based on the Cassinian oval (cf. Funaki [5] and Angelov and Mladenov [1]). This approach has the advantages traced by the simplicity of the model, the exact expressions that can be derived with either explicit or implicit coordinates (considered in Section 2) for the fundamental forms and curvatures (in Section 3), and other essential differential-geometric quantities, such as volume and surface area (see Section 4). Besides, qualitative insight obtained for reduced volumes and reduced spontaneous curvature within the **Cassinian model of axisymmetric vesicles** (CAV) are directly translated in Section 5 to the previous results (cf. Seifert *et al.* [17]) for elastic bending energy at zero spontaneous curvature.

2. Vesicle Shapes Described by The Cassinian Oval Model

As explained in details elsewhere (cf. Funaki [5] and Angelov and Mladenov [1]), the shape of red blood cell can be modelled via the Cassinian oval given in Cartesian coordinates by the following implicit equation:

$$\left(a^2 + x^2 + y^2 + z^2\right)^2 - 4a^2\left(x^2 + y^2\right) = c^4, \tag{2.1}$$

where the focus distance $2a$, and the extra free parameter c are real numbers. Let us introduce instead of a^2 the real number $\alpha \in \mathbb{R}$. Then the surface Eq. (2.1) becomes

$$\left(\alpha + x^2 + y^2 + z^2\right)^2 - 4\alpha\left(x^2 + y^2\right) = c^4. \tag{2.2}$$

In the case $\alpha > 0$ this equation is exactly the same as Eq. (2.1), but for $\alpha < 0$ it corresponds to a Cassinian oval with a focus distance which is a pure imaginary number. From now on we shall consider Eq. (2.2) as a basic model for the approximate analytical description of the axisymmetric vesicle shapes.

However, for a real differential–geometric description one needs also the explicit coordinates of the surface given by Eq. (2.2). Using the parametrization by spherical polar coordinates presented in Section 2.2 in Angelov and Mladenov [1], we can write:

$$x(\rho, \phi) = \sqrt{\frac{\left(\rho^2 + \mathring{x}^2\right)\left(\rho^2 - \mathring{z}^2\right)}{2\left(\mathring{x}^2 - \mathring{z}^2\right)}} \cos \phi$$

$$y(\rho, \phi) = \sqrt{\frac{\left(\rho^2 + \mathring{x}^2\right)\left(\rho^2 - \mathring{z}^2\right)}{2\left(\mathring{x}^2 - \mathring{z}^2\right)}} \sin \phi \tag{2.3}$$

$$z(\rho, \phi) = \pm \sqrt{\frac{\left(\mathring{x}^2 - \rho^2\right)\left(\mathring{z}^2 + \rho^2\right)}{2\left(\mathring{x}^2 - \mathring{z}^2\right)}}, \qquad \phi \in [0, 2\pi]$$

where $\mathring{x} = \sqrt{c^2 + \alpha}$, $\mathring{z} = \sqrt{c^2 - \alpha}$ and $\rho \in [\sqrt{c^2 - |\alpha|}, \sqrt{c^2 + |\alpha|}]$, while the positive (negative) sign for the third coordinate corresponds to that part of the surface that is above (below) the polar plane.

In Figure 1, the contour of the modified Cassinian oval in the first quadrant along with the intervals of $\mathring{x}$ and $\mathring{z}$ in corresponding directions are drawn. Here, the choice of spherical polar coordinates is motivated, at first by their convenience, and second for making more easy the comparison with representation of Liu *et al.* [13] in these coordinates.
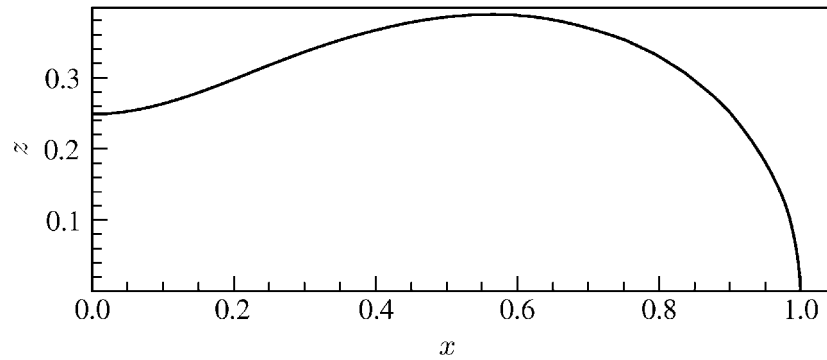

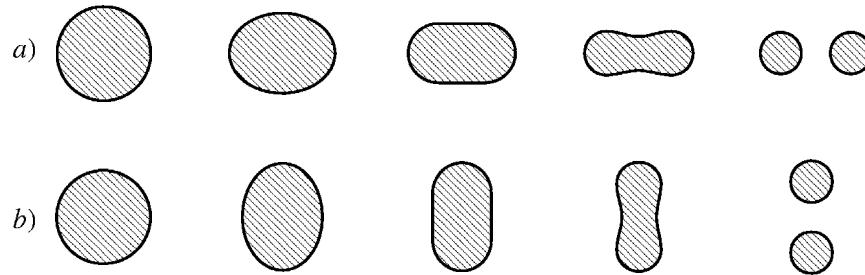**Figure 1.** Axisymmetric vesicle contour in the first quadrant

Figure 2. Various contours at different values of α

(*a*) Oblate branch: shapes for $\alpha \geq 0$; (*b*) Prolate branch: shapes for $\alpha \leq 0$

Figure 2*a*, shows contours for positive values of α that are plotted using Eq. (2.2) in the $x-z$ plane, i. e., $y = 0$. The corresponding shapes continuously change in the following sequence:

Spheres $\Rightarrow$ Oblate Ellipsoids $\Rightarrow$ Discocytes $\Rightarrow$ Red Blood Cells $\Rightarrow$ Torocytes

Figure 2*b* shows the corresponding contours for $\alpha \leq 0$. The shapes sequence is as follows:

Spheres $\Rightarrow$ Prolate Ellipsoids $\Rightarrow$ Capped Cylinders $\Rightarrow$ Dumb-Bells $\Rightarrow$ 2 Spheres

It is worth to mention that another classes of rotationally symmetric vesicles like stomatocytes and pears do not fall in the considered model. They can be modeled approximately within computer aided design (CAD) approach as explained in Bloor and Wilson [2].

The different shapes produced by Eq. (2.2) can be generated also by introducing the parameter

$$\omega = \frac{\mathring{x}^2 - \mathring{z}^2}{\mathring{x}^2 + \mathring{z}^2} = \frac{\alpha}{c^2} \,. \tag{2.4}$$

which is a generalization of the dimensionless ratio $\epsilon = a/c$, used previously in [1]. Further on we would call this dimensionless ratio a form or shape parameter. Range interval in which ω takes its values is just $[-1, 1]$.

3. Fundamental Forms and Curvatures of CAV

Using the standard notation in differential geometry textbooks (cf. e. g. Oprea [14]), the elements of the First Fundamental Form of the surface (2.1) are found to be:

$$E = -\frac{\rho^4 (\mathring{x}^2 + \mathring{z}^2)^2}{(\rho^4 - \mathring{x}^4)(\rho^4 - \mathring{z}^4)}, \quad F = 0, \quad G = \frac{(\rho^2 + \mathring{x}^2)(\rho^2 - \mathring{z}^2)}{2(\mathring{x}^2 - \mathring{z}^2)} \,. \tag{3.1}$$

The corresponding coefficients of its Second Fundamental Form are also needed, and the derived expressions are:

$$L = -\frac{\rho (\mathring{x}^2 + \mathring{z}^2)(3\rho^4 - \mathring{x}^2 \mathring{z}^2)}{(\rho^4 - \mathring{x}^4)(\rho^4 - \mathring{z}^4)} \,,$$

$$M = 0 \,, \tag{3.2}$$

$$N = \frac{(\rho^2 + \mathring{x}^2)(\rho^2 - \mathring{z}^2)(2\rho^2 - \mathring{x}^2 + \mathring{z}^2)}{2\rho (\mathring{x}^4 - \mathring{z}^4)} \,.$$

Since the coordinate directions coincide with the principal directions, i. e. we are working in a principal patch on the surface where $F = M = 0$, the respective principal curvatures can be expressed quite simply by the formulae (cf. Henderson [8]):

$$k_1 = \frac{L}{E} = \frac{3\rho^4 - \mathring{x}^2 \mathring{z}^2}{\rho^3 (\mathring{x}^2 + \mathring{z}^2)} \,, \tag{3.3}$$

$$k_2 = \frac{N}{G} = \frac{2\rho^2 - \mathring{x}^2 + \mathring{z}^2}{\rho (\mathring{x}^2 + \mathring{z}^2)} \,. \tag{3.4}$$

Now we can calculate the two most fundamental quantities of the surface under consideration, namely its **Gaussian**

$$K = \mathbf{k}_1 \cdot \mathbf{k}_2 = \frac{\left(2\rho^2 - \mathring{x}^2 + \mathring{z}^2\right)\left(3\rho^4 - \mathring{x}^2\mathring{z}^2\right)}{\rho^4\left(\mathring{x}^2 + \mathring{z}^2\right)^2} \tag{3.5}$$

and **mean**

$$H = \frac{1}{2}(\mathbf{k}_1 + \mathbf{k}_2) = \frac{5\rho^4 - \mathring{x}^2\mathring{z}^2 - \rho^2\left(\mathring{x}^2 - \mathring{z}^2\right)}{2\rho^3\left(\mathring{x}^2 + \mathring{z}^2\right)} \tag{3.6}$$

curvatures.

Finally, taking the square root of the determinant of the metric tensor, the surface area element can be obtained as:

$$\mathrm{d}A = \sqrt{EG}\,\mathrm{d}\rho \wedge \mathrm{d}\phi = \frac{\rho^2\left(\mathring{x}^2 + \mathring{z}^2\right)}{\sqrt{2(\rho^2 - \mathring{x}^2)(\rho^2 + \mathring{z}^2)(\mathring{z}^2 - \mathring{x}^2)}}\,\mathrm{d}\rho \wedge \mathrm{d}\phi. \tag{3.7}$$

4. Volume, Surface Area, and Homogeneity index of CAV

For axisymmetric case, the geometric quantities, such as volume V and surface area A, can be expressed in a form relevant to the sphere (cf. Angelov and Mladenov [1], Heinrich *et al.* [6]), by ascribing a correction (or effective) factor that depends only on the form parameter (Eq. (2.4)). This property is related to the scale invariance of the elastic energy of bending of lipid bilayer membrane that forms the vesicle (Peliti [16], Seifert *et al.* [17]).

4.1. Volume

The volume V of our model vesicles can be expressed in analogous way as in Angelov and Mladenov [1]. Using the shell method we obtain after integration the following results:

$$V(\omega) = \frac{4}{3}\pi\mathring{z}^3 V_-(\omega) \quad \text{for } \omega < 0, \tag{4.1}$$

and

$$V(\omega) = \frac{4}{3}\pi\mathring{x}^3 V_+(\omega) \quad \text{for } \omega > 0, \tag{4.2}$$

where the dimensionless effective factors of $V(\omega)$ are

$$V_-(\omega) = \frac{1 + 2\omega}{4(1 - \omega)} - \frac{3\log(1 + 2\sqrt{\omega(\omega - 1)}) - 2\omega)}{8\sqrt{\omega}(\omega - 1)^{\frac{3}{2}}} \tag{4.3}$$

$$V_+(\omega) = \frac{\sqrt{1-\omega}\,(1+2\omega)}{4(1+\omega)^{\frac{3}{2}}} + \frac{3\arccos(1-2\omega)}{8\sqrt{\omega}(1+\omega)^{\frac{3}{2}}}.$$ (4.4)
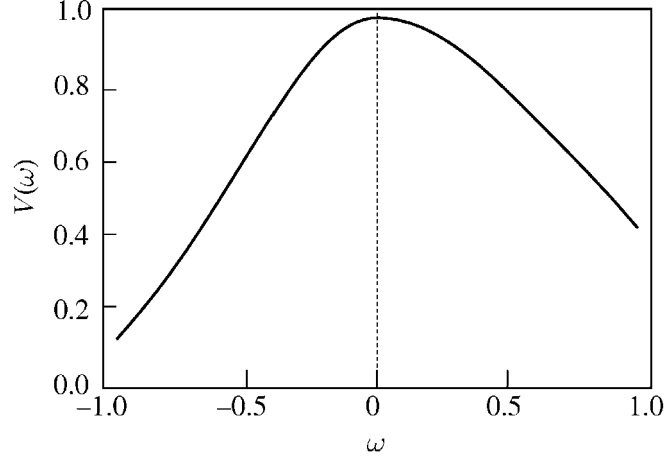
Figure 3 shows the plot of $V(\omega)$ *vs* ω.

Figure 3. Effective volume $V(\omega)$ *vs* the shape parameter ω

4.2. Surface Area

The surface area A was obtained integrating the surface area element from Eq. (3.7), i. e., $A = \int \mathrm{d}A$. Thus,

$$A(\omega) = 4\pi\mathring{z}^2 A_-(\omega) \quad \text{for } \omega < 0,$$ (4.5)

and

$$A(\omega) = 4\pi\mathring{x}^2 A_+(\omega) \quad \text{for } \omega > 0,$$ (4.6)

where the effective factors now are

$$A_-(\omega) = \frac{E\left(\frac{\omega+1}{\omega-1}\right) - E\left(\arcsin\sqrt{\frac{1-\omega}{1+\omega}}, \frac{\omega+1}{\omega-1}\right)}{\sqrt{\omega(1-\omega)}}$$

$$+ \frac{F\left(\arcsin\sqrt{\frac{1-\omega}{1+\omega}}, \frac{\omega+1}{\omega-1}\right) - K\left(\frac{\omega+1}{\omega-1}\right)}{\sqrt{\omega(1-\omega)}}$$ (4.7)

$$A_+(\omega) = \frac{E\left(\arccos\sqrt{\frac{1-\omega}{1+\omega}}, \frac{1+\omega}{2}\right) - \frac{1-\omega}{2}F\left(\arccos\sqrt{\frac{1-\omega}{1+\omega}}, \frac{1+\omega}{2}\right)}{(1+\omega)\sqrt{\omega/2}}$$ (4.8)

Here $F(\psi, k)$ and $E(\psi, k)$ denote the first, and respectively the second kind of incomplete elliptic integrals, while $K(k)$ and $E(k)$ denote the corresponding complete elliptic integrals. Their definition and properties can be found e. g. in Jahnke *et al.* [10]. Figure 4 shows the plot of $A(\omega)$ *vs* ω.
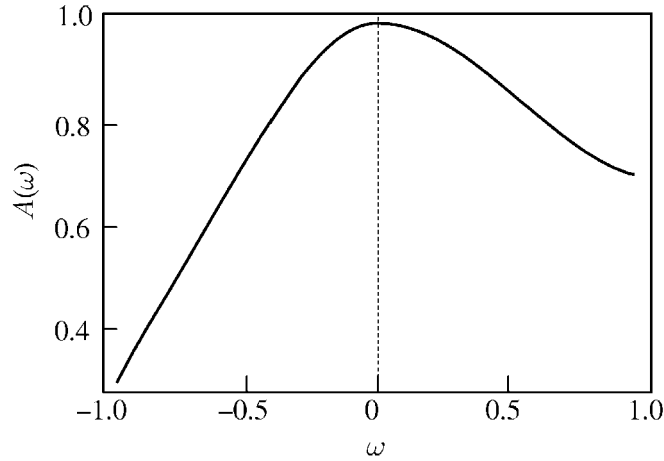

Figure 4. Effective area $A(\omega)$ *vs* shape parameter ω

4.3. Homogeneity Index and Volume at Constant Surface Area

Since A can be written as $4\pi R^2 A(\omega)$, it follows that

$$R^2 = \frac{A}{4\pi A(\omega)}.$$ (4.9)

On the other side $V = \frac{4}{3}\pi R^3 V(\omega)$, and consequently

$$V = \frac{A^{\frac{3}{2}} V(\omega)}{6\sqrt{\pi}A(\omega)^{\frac{3}{2}}} = \frac{A^{\frac{3}{2}}}{6\sqrt{\pi}\text{HI}},$$ (4.10)

where the homogeneity index HI is given by (cf. Hyde *et al.* [9], p. 151)

$$\text{HI} = \frac{A^{\frac{3}{2}}}{6\sqrt{\pi}V} = \frac{A(\omega)^{\frac{3}{2}}}{V(\omega)}.$$ (4.11)

Therefore the homogeneity index is a function only of the shape parameter ω. If $A = \text{const}$, i. e., the surface area of the vesicle is constant and do not changes, Eq. (4.10) gives direct relation between the vesicle volume v at constant surface area and the homogeneity index. For example, let $A^{\frac{3}{2}} = 6\sqrt{\pi}$, then the volume will be $v = 1/\text{HI}$. Usually, the volume at constant surface area is referred as reduced (Deuling and Helfrich [4]) or relative volume (Kralj-Iglič *et al.* [12]). Figure 5 shows a plot of the reduced volume $v(\omega)$ and the homogeneity index $\text{HI}(\omega)$ *vs* ω.
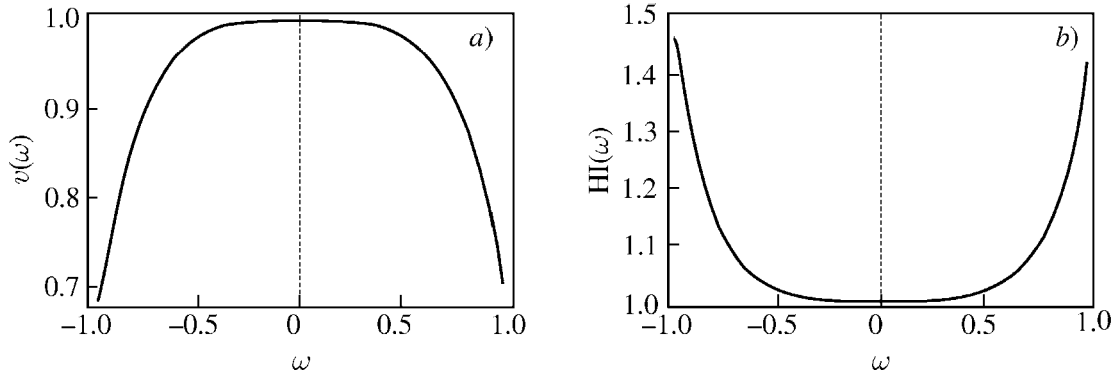
Figure 5. Reduced volume $v(\omega)$ and homogeneity index $\text{HI}(\omega)$ *vs* shape parameter ω

Constant surface area was initially used by Canham [3] to account for the constant number of lipid molecules in the vesicle membrane. From the point of view of the thermodynamics, the homogeneity index here would be proportional to the concentration of lipid molecules included in the vesicle volume.

5. Elastic Energy of Bending of CAV

5.1. Elastic Energy of Bending

The bending energy, within Canham model [3] of elasticity of lipid membranes, is given by the following formula:

$$F = 2k \int H^2 \, dA, \tag{5.1}$$

where k is the elastic modulus of the membrane, H is the mean curvature of the membrane (cf. Eq. (3.6)), and integration is over the surface area of the vesicle. It is known that the elastic energy of bending is a scale invariant (Seifert *et al.* [17]), and this was checked directly for the Cassinian oval in [1]. Soon after Canham's work, the expression for bending energy was modified by Helfrich [7] in order to account the possible asymmetry of the lipid bilayer, and based on argumentation from elastic theory of liquid crystals. This is furnished by introduction of the so called spontaneous curvature lh,

$$F = \frac{k}{2} \int (2H - \text{lh})^2 \, dA. \tag{5.2}$$

In the case of CAV model, we could write bending energy using Eq. (3.6), and Eq. (3.7),

$$F(\omega) = \frac{k}{2} F_-(\omega, \text{lh}), \quad \text{if} \quad \omega < 0 \tag{5.3}$$

and

$$F(\omega) = \frac{k}{2} F_+(\omega, \mathrm{lh}), \quad \text{if} \quad \omega > 0, \tag{5.4}$$

where

$$F_-(\omega, \mathrm{lh}) = \frac{\pi}{\sqrt{\omega}} \int_1^{\sqrt{\frac{1+\omega}{1-\omega}}} \frac{\left(5(1-\omega)\rho^4 - 2\mathrm{lh}\rho^3 - 2\omega\rho^2 - \omega - 1\right)^2}{\rho^4 \sqrt{((\omega-1)\rho^2 + \omega + 1)(1+\rho^2)}} \, d\rho,$$

$$\tag{5.5}$$

$$F_+(\omega, \mathrm{lh}) = \frac{\pi}{\sqrt{\omega}} \int_{\sqrt{\frac{1-\omega}{1+\omega}}}^1 \frac{\left(5(1+\omega)\rho^4 - 2\mathrm{lh}\rho^3 - 2\omega\rho^2 + \omega - 1\right)^2}{\rho^4 \sqrt{((\omega+1)\rho^2 - \omega + 1)(1-\rho^2)}} \, d\rho.$$

When $\mathrm{lh} = 0$, it can be proved that $F_-(-|\omega|, 0) = F_+(|\omega|, 0)$. Bending energy $F(\omega)$ as a function of the shape parameter ω for $\mathrm{lh} = 0$ is shown in Fig. 6.
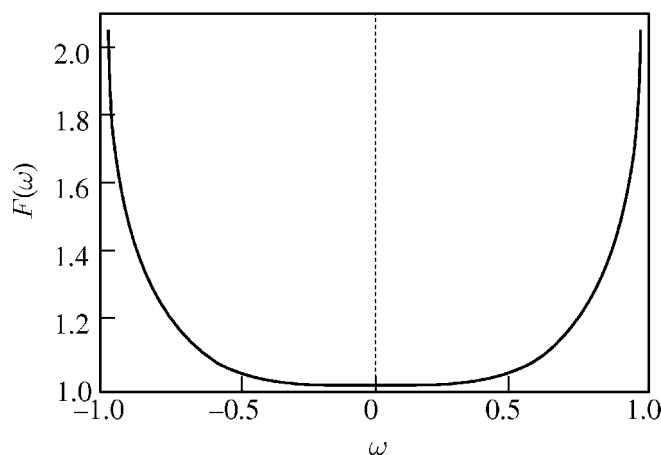

Figure 6. Bending energy $F(\omega)$ *vs* shape parameter ω

5.2. Bending Energy versus Reduced Volume and Non Zero Spontaneous Curvature

In analogical way to phase diagrams of $\mathrm{Lipid}_c/\mathrm{Water}_{1-c}$ systems, the phase diagrams of vesicles represent the minimum of elastic bending energy as a function of spontaneous curvature and reduced volume (cf. Canham [3], Seifert *et al.* [17] and p. 116 in Hyde *et al.* [9]). In CAV model the relation between reduced volume and shape parameter can be derived in analytical form, and phase diagram could be constructed in terms of the natural variables (ω, lh), but we will not follow this way. Instead, we follow the tradition and make use of the variables (v, lh). In Figure 7 the elastic bending energy is plotted as a function of reduced volume for negative, zero and positive spontaneous

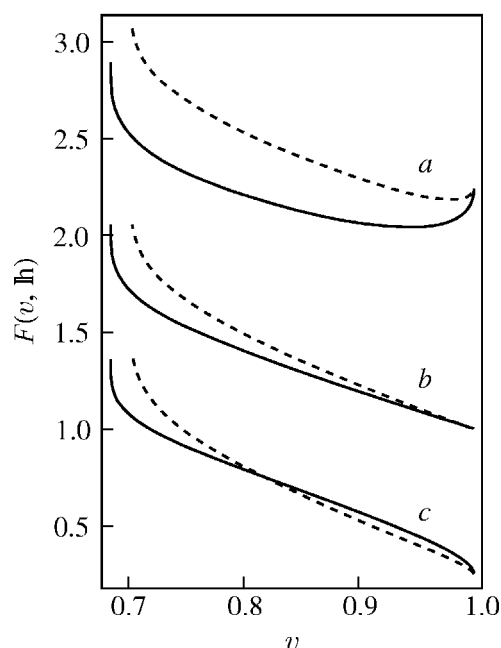curvatures. It is instructive to note that CAV model produces similar results to spontaneous curvature model.

Figure 7. Bending energy $F(v, \text{lh})$ *vs* reduced volume v and spontaneous curvature: (*a*) $\text{lh} = -1$, (*b*) $\text{lh} = 0$, and (*c*) $\text{lh} = 1$ Unbroken lines correspond to prolate branch, dashed lines — to oblate branch

6. Concluding Remarks

We have shown that Cassinian oval model of vesicles gives relatively simple analytical results for the geometric quantities and bending energy that are necessary for building vesicle phase diagram. CAV model is directly comparable to exact numerical results of spontaneous curvature model, which makes both models more clear and valuable. We hope also that calculations in this paper could be used as a guide for searching new exact solutions of vesicle shape equation or its alternatives based on generalization of the Laplace equation [11].

Acknowledgments

References

[1] Angelov B. and Mladenov I., *On The Geometry of Red Blood Cell*, In: Geometry, Integrability and Quantization, (I. Mladenov and G. Naber, Eds), Coral Press, Sofia 2000 pp 27–46.

[2] Bloor M. and Wilson M., *Method for Efficient Shape Parametrization of Fluid Membranes and Vesicles*, Phys. Rev. E **61** (2000) 4218–4229.

[3] Canham P. *The Minimum Energy of Bending as a Possible Explanation of the Biconcave Shape of the Human Red Blood Cell*, J. Theor. Biol. **26** (1970) 61–81.

[4] Deuling H. and Helfrich W., *Red Blood Cell Shapes as Explained on the Basis of Curvature Elasticity*, Biophys. J. **16** (1976) 861–868.

[5] Funaki H., *Contribution on the Shapes of Red Blood Corpuscles*, Japan. J. Physiol. **5** (1955) 81–92.

[6] Heinrich V., Božič B., Svetina S. and Žekš B., *Vesicle Deformation by an Axial Load*, Biophys. J. **76** (1999) 2056–2071.

[7] Helfrich W., *Elastic Properties of Lipid Bilayers*, Z. Naturforsch. **28c** (1973) 693–703.

[8] Henderson D., *Differential Geometry: A Geometric Introduction*, Prentice Hall, New Jersey 1998.

[9] Hyde S., Anderson S., Larson K., Blum Z., Landh T., Lidin S. and Ninham B., *The Language of Shape*, Elsevier 1997.

[10] Jahnke E, Emde F. and Lösch F., *Tafeln Höherer Funktionen*, Teubner Verlag, Stuttgart 1960.

[11] Kralchevsky P. A., Eriksson J. C. and Ljunggren S., *Theory of Curved Interfaces and Membranes: Mechanical and Thermodynamical Approaches*, Advances in Colloid and Interface Science **48** (1994) 19–59.

[12] Kralj-Iglič, V., Iglič A., Hagerstrand H. and Peterlin P., *Stable Tubular Microexovesicles of the Erythrocyte Membrane Induced by Dimeric Amphiphiles*, Phys. Rev. E **61** (2000) 4230–4234.

[13] Liu Q.-H., Z. Haijun J.-X. Liu and Ou-Yang Zhong-Can, *Spheres and Prolate and Oblate Ellipsoids from an Analytical Solution of Spontaneous Curvature Fluid Membrane Model*, Phys. Rev. E **60** (1999) 3227–3233.

[14] Oprea J., *Differential Geometry and Its Applications*, Prentice Hall, New Jersey 1997.

[15] Ou-Yang Zhong-Can, Liu Ji-Xing and Xie Yu-Zhang, *Geometric Methods in The Elastic Theory of Membranes in Liquid Crystal Phases*, World Scientific, Singapore 1999.

[16] Peliti L., *Amphiphilic Membranes*, In: Fluctuating Geometries in Statistical Mechanics and Field Theory, (F. David, P. Ginsparg and J. Zinn-Justin, Eds), Les Houches Session LXII, 1994, Elsevier, Amsterdam 1996 pp 195–285.

[17] Seifert U., Berndl K. and Lipowsky R., *Shape Transformations of Vesicles: Phase Diagram for Spontaneous-Curvature and Bilayer-Coupling Models*, Phys. Rev. A**44** (1991) 1182–1202.

[18] Seifert U. and Lipowsky R., In: *Handbook of Biological Physics Vol. 1*, (R. Lipowsky and E. Sackmann, Eds), Elsevier, Amsterdam 1995.